Photoluminescence of an Yb^{3+}/Al^{3+}-codoped microstructured optical fibre*

Xia Chang-Ming(夏长明)[a)b)], Zhou Gui-Yao(周桂耀)[a)b)†], Han Ying(韩 颖)[a)], and Hou Lan-Tian(侯蓝田)[a)]

[a)] *State Key Laboratory of Metastable Materials Science and Technology, Yanshan University, Qinhuangdao* 066004, *China*

[b)] *School of Information and Optoelectronic Science and Engineering, South China Normal University, Guangzhou* 510006, *China*

(Received 7 March 2011; revised manuscript received 18 April 2011)

An Yb^{3+}/Al^{3+}-codoped microstructured optical fibre is prepared based on photonic crystal fibre technology. The characteristic spectra of preforms and fibres are experimentally investigated. The results show that under a 971 nm excitation, besides the known infrared fluorescence luminescence around 1050 nm, a blue luminescence peak at 486 nm is obtained. Moreover, an unexpected emission peak at 730 nm is also observed. The photoluminescence mechanism of an Yb^{3+}/Al^{3+}-codoped microstructured optical fibre is discussed. The emission peak at 486 nm is attributed to the cooperative upconversion resulting from pairs of Yb^{3+} ions, and the emission peak around 730 nm is ascribed to the stimulated Raman scattering because of nonlinear effects of microstructured optical fibre. The Yb^{3+}/Al^{3+}-codoped microstructured optical fibre is promising for varieties of applications from laser printing and optical recording to cancer treatments, such as photodynamic therapy.

Keywords: photoluminescence, Yb^{3+}/Al^{3+}-codoped, microstructured optical fibre

PACS: 78.55.–m, 42.81.–i, 73.61.Jc **DOI:** 10.1088/1674-1056/20/8/087802

1. Introduction

In recent years, upconversion luminescence has been one of the most interesting topics.[1−3] It offers an attractive opportunity to develop ultraviolet and visible light sources. Some studies have demonstrated that the upconversion luminescence emission is existent in the rare earth (RE) doped glass materials.[4] Investigations into Yb^{3+}-doped materials have revealed that Yb^{3+} ions can produce not only laser emission in the near infrared region from 900 nm to 1200 nm but also narrow and bright visible emission around 486 nm due to cooperative upconversion emission.[5,6] Cooperative upconversion luminescence is a special type of upconversion luminescence.[7] In the Yb^{3+} system, two interacting ions in the excited state can emit one photon when they return to the ground state simultaneously, while the energy of the output photon is twice the energy of the single ion transition. Therefore, more and more attention has been paid recently to investigation of the upconversion luminescence of Yb^{3+} ions. In 2001, Chen *et al.*[1] reported blue upconversion luminescence at 479.5 nm in Yb^{3+}-doped oxyfluoride vitroceramics. In 2005, Xu *et al.*[4] reported upconversion luminescence performed in Yb^{3+}-doped yttrium aluminum garnets. In 2008, Wang *et al.*[8] reported strong blue cooperative up-conversion emission around 475 nm in Yb^{3+}-doped hexagonal $NaYF_4$. The Yb^{3+}-doped microstructure optical fibres (MOFs) have been reported and used to develop high power lasers. Furthermore, the nonlinear effects of MOFs, such as frequency doubling and upconversion, have also been used to develop ultraviolet and visible light sources.[9,10] However, there are also few reports of the cooperative upconversion luminescence effects in Yb^{3+} and Yb^{3+} activated silica fibres.

In the present paper, we fabricate an Yb^{3+}/Al^{3+}-codoped MOF based on photonic crystal fibre technology. The characteristic spectra of Yb^{3+}/Al^{3+}-codoped MOF are experimentally investigated. The photoluminescence mechanism in our Yb^{3+}/Al^{3+}-codoped MOF is discussed thoroughly.

*Project supported by the State Key Program of National Natural Science Foundation of China (Grant No. 60637010) and the Major Basic Research Development Program of China (Grant No. 2010CB327604).

†Corresponding author. E-mail: zguiyao@163.com

© 2011 Chinese Physical Society and IOP Publishing Ltd

2. Experiment

The Yb^{3+}/Al^{3+}-codoped MOF used in this work is prepared based on photonic crystal fibre technology.[11,12] Fabrication of RE-doped MOF can generally be divided into three steps: the fabrication of the core preform, the fabrication of the fibre perform, and the drawing of the preform into a fibre. First, the Yb^{3+}-doped SiO_2–Al_2O_3 glass is successfully prepared by the solution doping process and the high temperature melting method. Here, Al^{3+} prevents rare earth ions from clustering and raises the solubility of Yb^{3+} ions; moreover, co-doped alumina is of the recommended amount for the best fluorescence lifetime. The 99.9999% (SiO_2) and 99.99% (other components) pure raw materials are appropriately weighed according to a specific weight ratio. After the compounds are ground, they are mixed in the solution process. After removing H_2O, the powder is sintered into glass at a high temperature (1950 °C). Then the glass samples are cut and optically polished into 2 mm × 2.7 mm × 5 cm for the measurement. Secondly, microstructured preforms are formed by stacking a number of capillary silica tubes and rods to form the desired air/silica structure. The core of the microstructured preform is substituted by the Yb^{3+}-doped glass rod mentioned above. It is noted that the silica cladding layer of the traditionally doped fibre core area introduced by the traditional modified chemical vapour deposition (MCVD)[13−16] technology is removed in our process. The MCVD is a process in which the silica soot is deposited on the inner surface of silica glass tube. After deposition, the silica glass tube is difficult to remove, so there appears the silica glass cladding layer in doped fibre core area. Finally, when the Yb^{3+}-doped microstructured preform has been constructed, it is drawn into a fibre in a normal fibre drawing tower under a high temperature (1800 °C). The UV-vis/NIR absorption spectra of the glass are recorded between 200 nm and 1100 nm by an AvaSpec-2048-USB2 spectrometer. The emission spectrum of the fibre is obtained between 200 nm and 1100 nm upon excitation of 971 nm with an AvaSpec-2048-USB2 spectrophotometer. An InGaAs laser diode and a Ti:Al_2O_3 laser (Mirra 900, Coherent, USA) are used as the laser pump source. All the measurements are performed at room temperature.

3. Experimental results and analyses

3.1. Cross-section of microstructured optical fibre

Figure 1 shows a cross section of MOF prepared by the method mentioned above. Viewing from the transverse cross section, the refractive index of the fibre cladding structure is not strictly periodic. The final geometry of Yb^{3+}-doped MOF has a serious deviation from the ideal MOF because of the collapse of air holes in the fabrication process. Furthermore, there is a big Yb^{3+}-doped core (about several hundred micrometers) in the central area of the fibre, which provides the possiblity for the propagation of the high power laser pulse.

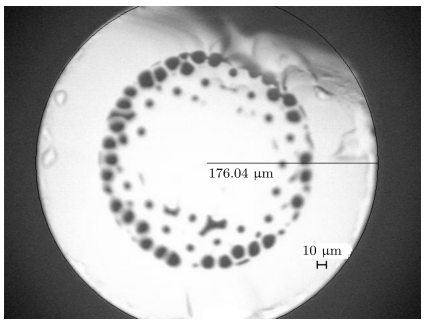


Fig. 1. The cross-section image of an Yb^{3+}/Al^{3+}-codoped MOF.

3.2. Absorption spectrum

Figure 2 shows the room temperature absorption spectrum of the proposed glass. From Fig. 2, we can see that the absorption spectrum is diffused in the 860 nm–1000 nm wavelength range. In addition, there are two significant absorption peaks appearing at 910 nm, 971 nm separately, which is not the same as the spectrum reported in Ref. [17]. What is interesting is that the absorption bandwidth and intensity of Yb^{3+}-ions at 910 nm are higher than those of 971-nm wavelength. This phenomenon in the Yb^{3+}-doped glass material is observed for the first time here, as far as we know. This appearance is related to the change in strength of the ligand field surrounding ions of dopants. Moreover, an interesting phenomenon is the observation of the new broad band near 384 nm in our spectrum. Su *et al.*[17] ascribed the ultraviolet absorption band of 384 nm to the $4f^{14}$–$4f^{13}5d^1$ transitions of Yb^{2+} ions. The first excited state levels ($4f^{13}5d^1$) of Yb^{2+} ions form $^2F_{7/2}(e_g)$, $^2F_{7/2}(t_{2g})$, $^2F_{5/2}(e_g)$, and

$^2F_{5/2}(t_{2g})$ states, and the ground state ($4f^{14}$) forms $^1S_0$ state. Therefore, the electronic transition from $^1S_0$ ground state to $^2F_{7/2}(e_g)$ excited states results in the absorption band peak at 384 nm.[18] According to the above analysis, this also indicates that Yb^{2+} ions and Yb^{3+} ions are coexisting states in our silica glass. Furthermore, we can also see that no self-absorption exists at a lasing wavelength of 1050 nm in the glass at room temperature.

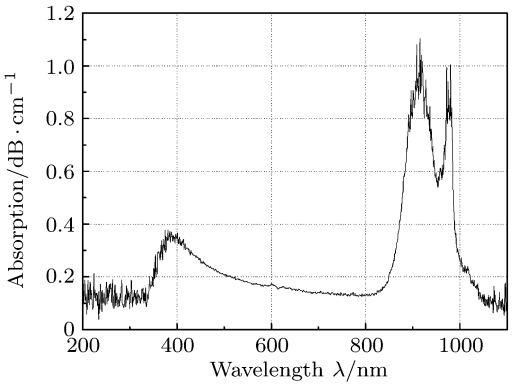


Fig. 2. Absorption spectrum of the Yb^{3+}/Al^{3+}-codoped glass at room temperature.

3.3. Emission spectrum

3.3.1. Emission spectrum under diode-laser excitation

Figure 3 shows the room temperature emission spectrum of the Yb^{3+}/Al^{3+}-codoped MOF under 971-nm excitation. Three distinct emission bands at 486, 512, and 837 nm from the visible to near infrared and a known fluorescence band at 1050 nm are observed (see the inset). The waveform within 400 nm–600 nm is the same as that reported in Ref. [6]. Xu *et al.*[4] have suggested that the blue emission band of 486 nm can result from the cooperative process corresponding to the simultaneous radiation relaxation of a pair of excited Yb^{3+} ions. This luminescent phenomenon can be well understood by the energy diagram, as shown in Fig. 4. The energy level scheme of the Yb^{3+} ion is simple with only the $^2F_{7/2}$ ground state and the $^2F_{5/2}$ excited state, separated by some 10000 cm^{-1}, and no energy level is in the visible region.[4] However, the 4f electrons of Yb^{3+} have a relatively strong interaction with their surroundings and the interaction between the $4f^{13}$ configurations of neighbouring Yb^{3+} is strong in comparison with those of other rare earth ions. The strong interaction gives rise to a high cooperative luminescence transition probability.[4] The visible photon emission of an excited Yb^{3+}–Yb^{3+} pair is in the following manner:[4,6]

$$Yb(^2F_{5/2}) + Yb(^2F_{5/2}) \rightarrow 2Yb\ (^2F_{7/2}) + h\nu.$$

The photon energy of the cooperative luminescence is nearly twice the energy of the normal (single-ion) luminescence. Therefore, it presents an absorption band of 486 nm here. The occurrence of the observed new broad band near 512 nm in the spectrum may be due to two possibilities behind this broad emission.[6] One originates from the Yb^{2+} state of Yb and the other comes from the defect centres caused by the doping of Yb^{2+} ions. However, in some host lattices, the Yb^{2+} luminescence is quenched such as aluminates, silicates and oxides.[19] So, we may draw the conclusion that the emission band of 512 nm is not caused by Yb^{2+} ions. The only cause is that the defect centres are introduced in the preparation process.[20] A small part of Yb^{3+} ions change their valences into Yb^{2+} ions in the preparation process of the glass because of the sintering environment effect. This case can be confirmed by the absorption spectrum. The absorption spectrum of the Yb^{3+}-doped glass (see Fig. 2) presents a characteristic absorption of Yb^{2+} ions, which shows that the valence states of Yb ions change from 3^+ valence to 2^+ valence in our glass. The variation of valence yields a colour centre around Yb^{2+} ions. The resulting colour centre may be responsible for broad upconversion emission spectrum at 512 nm. Moreover, Joshi *et al.*[6] have also suggested that the upconversion emission band in this wavelength region results from the defect centres. In our spectrum, the other interesting phenomenon is the observation of a new broad band near 837 nm. Though the detailed mechanism of this is still unknown, it is clear that the variation in luminescent properties can be ascribed to the nonlinear effects of MOF. According to the physics analysis, when an intense laser is launched into the fibre, MOF will generate high nonlinear effects, such as self-phase modulation (SPM), cross-phase modulation (CPM), stimulated Raman scattering (SRS), and stimulated Brillouin scattering (SBS) because of nonlinearity of fibre both in material and in structure. The emission peak at a wavelength of 837 nm is attributed to the nonlinear effect of the MOF, which still requires further study.

The absorbed near-infrared pump power dependence of upconversion luminescence is also investigated. By changing the diode-laser power from 1.6 W to 2.42 W, upconversion luminescence spectra are measured under a 971-nm excitation, as shown in Fig. 5. As expected, the spectrum intensity increases

with increasing pump power. However, there are observable changes neither in position nor in profile when the laser pump power is changed.

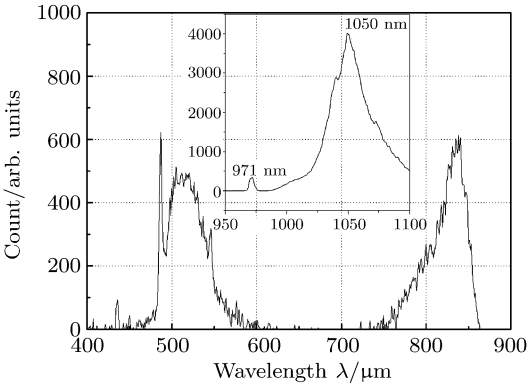


Fig. 3. Emission spectrum of Yb^{3+}-doped MOF under a 971-nm excitation by using the diode laser, with the inset showing 950 nm–1100 nm emission spectrum.

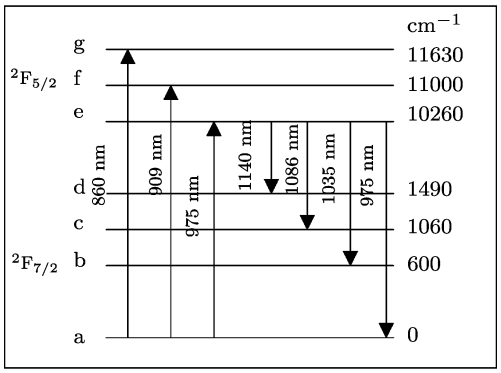


Fig. 4. Energy levels of Yb^{3+} ions.

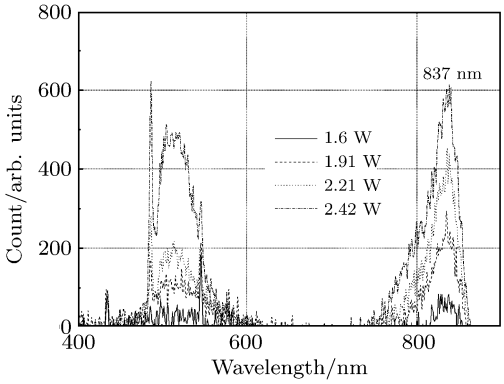


Fig. 5. Emission spectra, each as a function of laser pump power with 971 nm excitation by using the diode laser.

3.3.2. Emission spectrum under femtosecond laser excitation

Photoluminescence,[21] characteristic of the Yb^{3+}/Al^{3+} MOF pumped by an intense Ti:Al_2O_3 laser with a wavelength of 971 nm and a beam diameter of 0.8 mm, is also studied experimentally. Figure 6 shows that emission spectra within the 600 nm–1100 nm wavelength range, each as a function of laser pump power under a 971 nm excitation by using the femtosecond laser. Comparing Fig. 6 with Fig. 5, a big difference can be seen within 600 nm–1100 nm wavelength. There is an unexpected emission peak at 730 nm, which is not observed under a 971 nm excitation by using the diode laser. A high output power laser with 730 nm wavelength is needed for varieties of applications from laser printing and optical recording to cancer treatments, such as photodynamic therapy.[22] According to the analysis, the emission peak at 730 nm is ascribed to stimulated Raman scattering (SRS) because of the nonlinearity of MOF. As seen from the spectrum, much energy of the pumping light is transferred to awavelength of 730 nm when the MOF is excited by using the femtosecond laser.

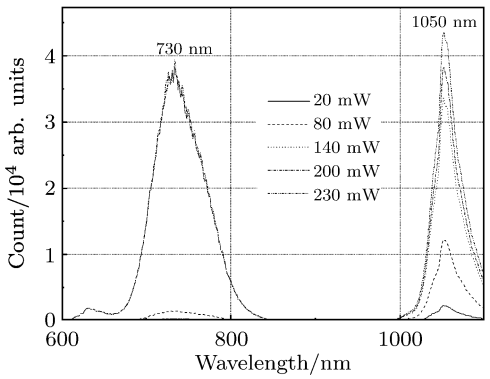


Fig. 6. Emission spectra, each as a function of laser pump power with 971 nm excitation by using the femtosecond laser.

Moreover, the intensity of the spectrum decreases with excitation wavelength increasing in this wavelength range, whose variation trend is contrary to that in the short wavelength range. According to the results, the anti-Stokes peak at a wavelength of 730 nm may be due to the nonlinear effect of the MOF. The nonlinear effect of the MOF is enhanced when the laser pulse is narrow by using the femtosecond laser excitation. The energy of the laser pulse is focused on a small area, which results in the quickly increase of the energy per unit area. As a result, the nonlinear effect of the MOF quickly increases. The anti-Stokes peak shifts toward short wavelengths when the Yb^{3+}/Al^{3+}-codoped MOF is excited by using an intense femtosecond laser pulse laser, which can explain why the strong anti-Stokes peak is at 730 nm wavelength under 971 nm excitation by using the intense femtosecond laser pulse

laser, while the anti-Stokes peak is at 837 nm wavelength under 971 nm excitation by using the diode laser. Moreover, under 971 nm excitation, the emission spectra within a 400 nm–600 nm wavelength, each as a function of the laser pump power, are also studied experimentally as shown in Fig. 7. The waveforms are the same as those of emission spectra generated under a 971 nm excitation by using the diode laser. However, the intensity of emission spectrum increases with increasing laser pump power.

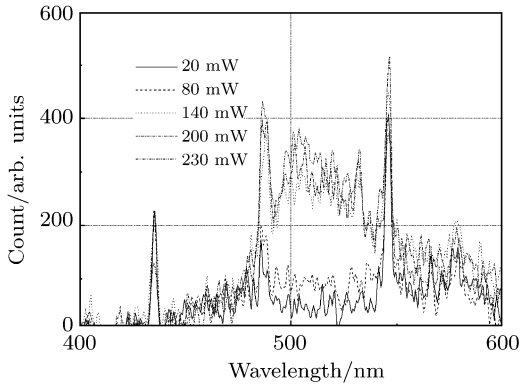


Fig. 7. Emission spectra within the 400 nm–600 nm wavelength range, each as a function of laser pump power with 971 nm excitation by using the femtosecond laser.

In addition, under 910, 919, 971 nm excitations, the emission spectra within the 400 nm–600 nm wavelength range are also studied experimentally, as shown in Fig. 8. The waveform does not change with excitation wavelength under the same laser pump power. However, the intensity of the spectrum increases with increasing excited wavelength. Figure 9 shows that emission spectra within the near-infrared wavelength range under 910, 919 and 971 nm excitations, separately. The waveform in the range 600 nm–1100 nm does not change with increasing excited wavelength either. However, the emission peak around the 730 nm wavelength shifts toward the shorter wavelengths, the peaks shift to 735 nm under 910 nm excitation, to 717 nm under 919 nm excitation, and to 713 nm under 971 nm excitation. The variation in the fluorescence emission peak at 1051 nm with increasing excited wavelength is the same as that of 730 nm wavelength. According to the results, the phenomenon can be explained by the absorption properties in our glass. The absorption band width and intensity at the wavelength of 910 nm are higher than those of the 971 nm wavelength. As can be seen from the absorption spectrum, efficient pumping is possible around a wavelength of 910 nm or near 971 nm. In the latter case, the pump linewidth must be small, and only a ∼50% excitation level can be achieved due to stimulated emission. Moreover, the absorption length and the quantum defect are bigger than those for 910 nm pumping. As a result, around a wavelength of 910 nm pumping is better for the absorption of the pumping energy. Strong three-level behaviour occurs for lasing around 1050 nm, where there is very little reabsorption. For ytterbium-doped materials, there is often a choice between different lasing transitions, where those with shorter wavelengths exhibit more pronounced three-level characteristics. According to the above analysis, the case where the emission peak around 730 nm shifts toward the shorter wavelengths may be due to the nonlinear effects of MOF, while the phenomenon that the emission peak around 1050 nm shifts toward the short wavelengths with the change in the excitation wavelength may be due to the change in the strength of the ligand field surrounding ions of the dopant.[23,24]

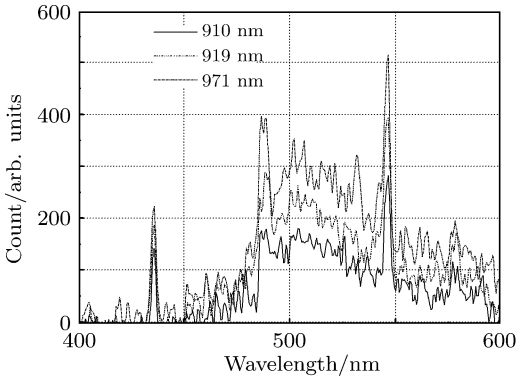


Fig. 8. Emission spectra within the 400 nm–600 nm wavelength range under 910, 919, 971 nm excitations by using the femtosecond laser.

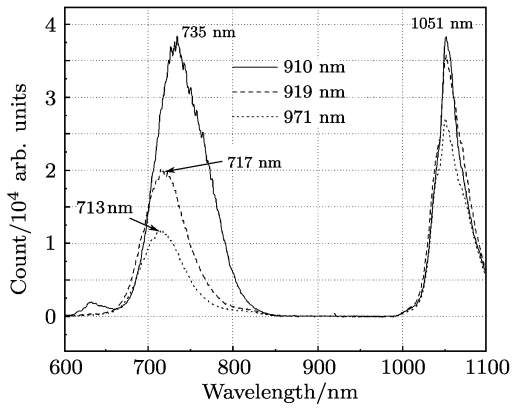


Fig. 9. Emission spectra within near-infrared wavelength range, under 910, 919, and 971 nm excitations by using the femtosecond laser.

4. Conclusion

We present experimental results describing the photoluminescence characteristics of Yb^{3+}/Al^{3+}-codoped MOF. The absorption spectrum shows that the absorption band width and intensity at a wavelength of 910 nm are higher than those of 971 nm wavelength in our Yb^{3+}-doped glass. To the best of our knowledge, this is the first observation phenomenon in the Yb^{3+}-doped materials, which opens a door for the study of the new optical properties in Yb^{3+}/Al^{3+}-codoped materials. Furthermore, three distinct emission bands at round 486, 512, and 837 nm from the visible to the near infrared and a known fluorescence band at round 1050 nm are observed, which provides a possibility for obtaining ultraviolet-to-visible light source. The emission peak at 486 nm is attributed to the cooperative upconversion resulting from pairs of Yb^{3+} ions, while the observation of a new broad band near 512 nm is due to the defect centres caused by the doping of Yb^{2+} ions. Under 971 nm excitation, there is an unexpected emission peak at 730 nm by using a femtosecond laser that is not observed by using the diode laser, thereby providing a platform for varieties of applications ranging from laser printing and optical recording to cancer treatments, such as photodynamic therapy.

References

[1] Chen X B, Masaaki O and Wang G W 2001 *Chin. J. Lasers* **10** 369

[2] Auzel F 2004 *Chem. Rev.* **104** 139

[3] Li C R, Dong B, Li L and Lei M K 2008 *Chin. Phys.* B **17** 224

[4] Xu X D, Zhao Z W, Song P X, Jiang B X, Zhou G Q, Xu J, Deng P Z, Bourdet G, Chanteloup J C, Zou J P and Fulop A 2005 *Physica* B: *Condens. Matter* **357** 365

[5] Cacho V D D, Kassab L R P, Oliveira S L D and Morimoto N I 2006 *Matter. Res.* **9** 21

[6] Joshi C, Kumar K and Rai S B 2010 *J. Fluoresc.* **20** 953

[7] Wei X T, Zhao J B, Chen Y H, Yin M and Li Y 2010 *Chin. Phys.* B **19** 077804

[8] Wang X F, Xiao S G, Yang X L and Ding J W 2008 *J. Mater. Sci.* **43** 1354

[9] Denoyer A, Levesque Y, Jandl S, Goldner P, Guillot-Noel O, Viana B, Thibault F and Pelenc D 2008 *J. Lumin.* **128** 1389

[10] Malinowski M, Kaczkan M, Piramidowicz R, Frukacz Z and Sarnecki J 2001 *J. Lumin.* **94–95** 29

[11] Zhou G Y, Hou Z Y, Li S G and Hou L T 2006 *Appl. Opt.* **45** 4433

[12] Zhou G Y, Hou Z Y, Li S G, Han Y and Hou L T 2007 *Acta Phys. Sin.* **56** 6846 (in Chinese)

[13] Petit V, Sekiya E H, Okazaki T, Bacus R, Barua P, Yao B, Ohsono K and Saito K 2008 *Proc. SPIE* **6998** 69980A-1

[14] Webb A S, Boyland A J, Standish R J, Yoo S, Sahu J K and Payne D N 2010 *J. Non-Cryst. Solids* **356** 848

[15] Tang F Z, McNamara P, Barton G W and Ringer S P 2008 *J. Non-Cryst. Solids* **354** 927

[16] Tang F Z, McNamara P, Barton G W and Ringer S P 2006 *J. Non-Cryst. Solids* **352** 3799

[17] Su L B, Xu J, Li H J, Wen L, Zhu Y Q, Zhao Z W, Dong Y J, Zhou G Q and Si J L 2005 *Chem. Phys. Lett.* **406** 254

[18] Yoo H S, Vaidyanathan S, Kim S W and Jeon D Y 2009 *Opt. Mater.* **31** 1555

[19] Lizzo S, Klein Nagelvoort E P, Erens R, Meijerink A and Blasse G 1997 *J. Phys. Chem. Solids* **58** 963

[20] Engholm M and Norin L 2007 in *Conference on Lasers and Electro-Optics/Quantum Electronics and Laser Science Conference and Photonic Applications Systems Technologies*, OSA Technical Digest (CD), Optical Society of America, paper JTuA61

[21] Wang X H and Zhou Y H 2009 *Acta Phys. Sin.* **58** 4239 (in Chinese)

[22] Al-Muhanna A, Wade J K, Mawst L J and Fu R J 1998 *Appl. Phys. Lett.* **72** 641

[23] Mao Y L, Zhao Z W, Deng P Z and Gan F X 2004 *Acta Phys. Sin.* **53** 1524 (in Chinese)

[24] Hu L, Xu X W, Lu Z M, Fan Y, Li Y X and Tang C C 2010 *Chin. Phys.* B **19** 127807